β relaxation at the glass transition of hard-spherical colloids

W. Götze
Physik Department, Technische Universität München, D-8046 Garching, Federal Republic of Germany and Max-Planck-Institut für Physik und Astrophysik, D-8000 München, Federal Republic of Germany

L. Sjögren
Institute of Theoretical Physics, Chalmers University of Technology, S-412 96 Göteborg, Sweden
(Received 13 September 1990)

The glass transition studied for suspensions of colloidal particles through dynamical light-scattering experiments is analyzed within the mode-coupling theory for the supercooled liquid dynamics. These suspensions are treated as simple atomic systems with a hard-sphere interaction. The scaling properties predicted by the theory are verified. The shape of the master function for the β-relaxation region agrees well with the experimental data.

Suspensions of small colloidal spherical particles of equal size show structural and dynamical properties that have many features in common with those of simple atomic systems.[1,2] In particular, the interaction between the particles is of very short range, and may come close to that of an ideal hard-sphere system.[3–5] While a simple atomic one-component system rapidly crystallizes upon supercooling, a colloidal system can be brought to a metastable fluid or glassy state for several hours or days without crystallization taking place. The dynamical properties of the metastable fluid and glassy states can therefore be studied. Recent dynamical light-scattering studies in a colloidal system detected a glass transition at a critical packing fraction $\varphi_c = 0.560 \pm 0.005$,[6,7] and the results were in overall agreement with computer simulations[8] and theoretical calculations.[9,10] In dynamical light-scattering experiments one measures directly the normalized intermediate scattering function $\phi_q(t) = F_q(t)/S_q$, as a function of wave vector q and time t. Here S_q denotes the static structure factor. Since $\phi_q(t)$ is of primary concern in mode-coupling theories of the glass transition, and can be calculated for a simple hard-sphere system, light-scattering experiments on colloidal systems seem to be an ideal way to quantitatively test the predictions of this theory, without introducing any adjustable parameters. In the present paper, we will analyze the experimental results along this line. A detailed discussion of the experiment with a complete reference list can be found in the preceding paper.[11]

The density-correlation function can be rewritten in terms of a generalized longitudinal viscosity $M_q(z)$ as

$$\phi_q(z) = -1/\{z - \Omega_q^2/[z + M_q(z)]\} \ . \tag{1a}$$

Here enters the well-known characteristic frequency of the liquid dynamics: $\Omega_q = (q^2 v^2/S_q)^{1/2}$, where v denotes the thermal velocity. The viscosity M can be decomposed into two parts: $M_q(z) = \Omega_q^2[m_q^0(z) + m_q(z)]$, where $m_q^0(z)$ describes the details of the liquid dynamics on microscopic time scales. It deals essentially with uncorrelated binary collision events. The most important part of the theory is $m_q(z)$, which describes correlated processes and is expressed in terms of the correlation function itself:

$$m_q(t) = \tfrac{1}{2} \sum_{k,p} V(\mathbf{q}, \mathbf{kp}) \phi_{\mathbf{k}}(t) \phi_{\mathbf{p}}(t) \ . \tag{1b}$$

The vertex $V(\mathbf{q}, \mathbf{kp}) \geq 0$ is given by the structure factor S_q,[9,10] and is assumed to depend regularly on external control parameters.

The self-consistent solution of the closed nonlinear equations above gives an ideal ergodic to nonergodic transition at a sufficiently large packing fraction φ_c. Close to φ_c there appear two distinct relaxation processes, the α and β processes, for times t longer than a typical microscopic time t_0. The α process exists only on the liquid side and describes the decay of density fluctuations on the longest time scale τ_α. The β process exists on mesoscopic time scales between the microscopic and α regions. For this latter relaxation process the mode-coupling theory makes detailed and nontrivial predictions for the behavior of $\phi_q(t)$. Explicitly one finds[12]

$$\phi_q(t) = f_q^c + h_q c_\sigma g_\pm(t/t_\sigma) \ , \tag{1c}$$

valid for

$$t_0 \ll t \ll \tau_\alpha \ . \tag{1d}$$

These formulas imply a scaling behavior in the specified time region. The solution depends, through the correlation scale c_σ and the time scale t_σ, crucially on the distance from the transition point measured via the separation parameter σ,

$$\sigma = \varphi/\varphi_c - 1 \ . \tag{2}$$

So the glass and liquid states correspond to $\sigma \gtrless 0$, respectively. The scaling functions $g_\pm$, where $\pm$ refers to $\sigma \gtrless 0$, respectively, as well as the parameters f_q^c and h_q do not depend on the packing fraction in leading order. The result in (1c) also predicts a strict factorization between the wave vector and time or frequency dependencies. The

 ©1991 The American Physical Society

functions $g_\pm$ do not depend on q; the wave vector enters only in the nonergodicity parameter f_q^c and the amplitude factor h_q. The master functions $g_\pm$ satisfy the equation[12]

$$\mp\frac{1}{\zeta}+\zeta g_\pm^2(\zeta)+\lambda i\int_0^\infty d\tau\, e^{i\zeta\tau}g_\pm^2(\tau)=0\ , \tag{3}$$

where $\zeta=zt_\sigma$ and $\tau=t/t_\sigma$ are rescaled variables. The scaling function depends therefore only on the exponent parameter λ, which is characteristic for any particular system. This parameter is given by various wave-vector integrals over the coupling constants V in (1b), and can be calculated numerically for some simple systems. The solution of (3) is known for any value of λ.[13] We can also obtain explicit expressions for short and long rescaled times. In the former case one finds

$$g_\pm(\tau\ll 1)=1/\tau^a\ . \tag{4a}$$

For long rescaled times one gets

$$g_+(\tau\gg 1)=1/\sqrt{1-\lambda}\ , \tag{4b}$$

$$g_-(\tau\gg 1)=-B\tau^b\ , \tag{4c}$$

where $B>0$. The exponents a and b are given by the exponent parameter λ by way of

$$\lambda=\Gamma^2(1-a)/\Gamma(1-2a)=\Gamma^2(1+b)/\Gamma(1+2b)\ , \tag{5}$$

where $0<a<\frac{1}{2}$ and $0<b<1$. The time scale in (1) diverges algebraically with σ:

$$t_\sigma=1/\omega_\sigma=t_0/|\sigma|^{1/2a}\ , \tag{6a}$$

and the correlation scale shows a simple square root variation

$$c_\sigma=\sqrt{|\sigma|}\ . \tag{6b}$$

The behavior in (4a) implies that for short times on scale t_σ the relaxation is the same for the liquid and the glass. For longer times, there is a qualitative difference between these two states. On the liquid side the critical decay crosses over to a new algebraic decay which is the von Schweidler law

$$\phi_q(t)=f_q^c-h_qB(t/t'_\sigma)^b\ . \tag{7a}$$

The new time scale t'_σ is the predicted scale for the α-relaxation process and it is given by

$$t'_\sigma=1/\omega'_\sigma=t_0/|\sigma|^\gamma,\quad \gamma=\frac{1}{2a}+\frac{1}{2b}\ . \tag{7b}$$

The decay in (7a) can only hold for $t/t'_\sigma\ll 1$. For larger times on scale $t'_\sigma=\tau_\alpha$ the dynamics is ruled by the α process, which will be considered below. In the glass the scaling function decays to a constant for long times. Together with f_q^c this constant gives the full nonergodicity parameter or Debye-Waller factor for the glass,

$$f_q=f_q^c+h_q\sqrt{|\sigma|/(1-\lambda)}+O(\sigma). \tag{8}$$

The formulas above can now be compared with experimental results. For a hard-sphere system all relevant quantities have been calculated earlier. For the critical packing fraction one obtained the value $\varphi_c=0.52\pm0.01$.[9,10,14] The exponent parameter of the hard-sphere system is $\lambda=0.758$ which gives the exponents $a=0.301$, $b=0.545$.[14] The corresponding master functions are shown in Fig. 1. The critical value of the nonergodicity parameter f_q^c was calculated[9] and the amplitude factor h_q was also obtained.[14] Equation (3) is scale invariant and does not allow one to fix t_0. The latter depends smoothly on σ, and characterizes the overall scale for the dynamics outside the transient initial motion. It depends on the properties of the solvent and on the coupling of the particles via hydrodynamic interactions. It has to be determined via matching of the general β-relaxation solution to the transient dynamics. The latter is not known in detail and therefore the one number t_0 enters the following analysis as fit parameter. It connects the mathematical time with the physical one. Let us emphasize here that β relaxation is used in the present context as dynamics described by Eq. (1c). It contains also the initial part of the α process, as described by (7a); see below for a more detailed discussion.

Equation (1c) specifies an asymptotic solution for the mode-coupling equations valid in the limit $\sigma\to 0$ but $t/t_\sigma=\tau$ fixed. For $\sigma\neq 0$ one gets deviations from the scaling law. For $t\to t_0$, they depend on all the tranisient properties and cannot be calculated at present. For $t\to t'_\sigma$ the deviations are given by the master functions of the α process. The results for the latter are not yet available, but the following general features are known. $\phi_q(t)$ remains positive and therefore the von Schweidler asymptote falls below the correlation function for large times.

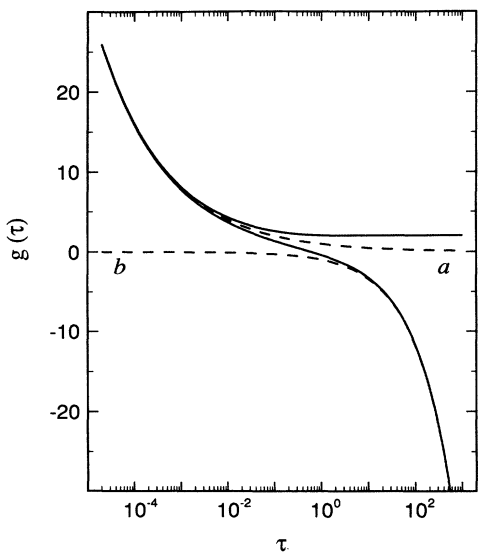

FIG. 1. Master functions for the hard-sphere system with exponent parameter $\lambda=0.758$ (solid curves). The dotted line, denoted by a, is the critical decay law $1/\tau^a$. The dotted line, denoted by b, is the von Schweidler law $-B\tau^b$. Here $a=0.301$, $b=0.545$, $B=0.963$. On the liquid side $g_-(\tau^*)=0$ for $\tau^*=0.608$.

The onset of this deviation of α process from β process depends on q; it occurs earlier and is stronger the smaller f_q^c. If f_q^c is large, i.e., for q near the peak position q_m of the structure factor, the part of $g_-(\tau)$ for $\tau > \tau^*$, where $g_-(\tau^*)=0$, is followed for a long interval. In this case deviations from scaling are big for $\tau < \tau^*$. If f_q^c is smaller, i.e., for q off the peak position q_m, the opposite holds. The part of $g(\tau)$ with $\tau < \tau^*$ is followed for a long interval, but a clearly developed von Schweidler law cannot be observed.[15]

The scaling behavior in (1c) implies that the experimental results for various values of φ should fall on the same master curves $g_\pm(\tau)$ provided the data for $\phi_q(t)-f_q^c$ are shifted with appropriate scale factors $h_q c_\sigma$ and t_σ. The best way to test this property is to separately test the shape of the experimental functions and the analytical form for the scales. In this way one can precisely compare with the predicted shape, Fig. 1, for the master functions and the analytical form for the scales. The result of such an analysis is shown in Fig. 2. The various symbols refer to the experimental light-scattering results;[11] to avoid overloading of the figure we have reproduced only ten experimental values per decade spaced with equal distance on the $\log(t)$ abscissa. The solid curves are the theoretical results. These latter curves were obtained in the following way. First one has to fix a value for the parameter f_q^c above. The predicted value for f_q^c is 0.87 ± 0.01.[9,14] This number for f_q was also measured for $\varphi=0.565$.[11] Since this value of φ refers to the glass state, the present value for f_q^c must be smaller than 0.87. This observation agrees with the general conclusion that the mode-coupling theory has some tendency to overestimate the trend to the glass formation and the structures in f_q.[14] This is, for instance, reflected in the calculated value $\varphi_c=0.52$ above,[9] which is lower than the observed value. We tried therefore with a 5% lower value $f_q^c=0.83$. Figure 2 shows the corresponding

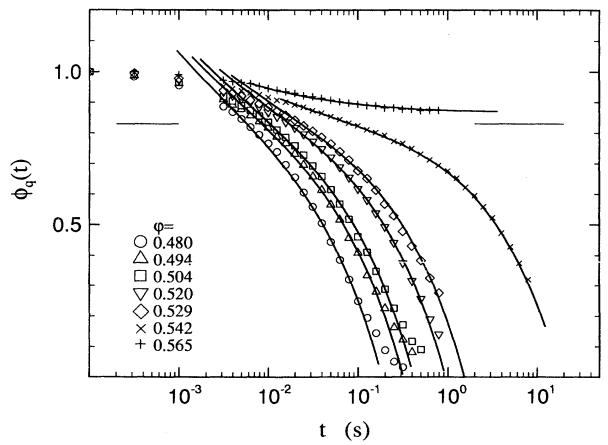

FIG. 2. Normalized intermediate scattering function $\phi_q(t)$ measured at the peak $q=q_m$ of the static structure factor (symbols). The solid curves are the predictions of the mode-coupling theory according to (1). The horizontal lines are drawn at $f_q^c=0.83$.

fit to be quite reasonable. Slightly different values might give somewhat better fits; but optimization in the choice of f_q has not been tried in order to avoid overinterpretation of the data. Having determined f_q^c we can now read off the values for the scaling times t_σ on the liquid side of the transition. These values are obtained from the times t_σ^* where $\phi_q(t_\sigma^*)=f_q^c$ or $g_-(t_\sigma^*/t_\sigma)=0$; for the present λ the zero τ^* of the master function, $g_-(\tau^*)=0$, is $\tau^*=0.608$. On the glassy side the scale t_σ can be fixed by fitting the critical spectrum for short times. The amplitude factor $h_q c_\sigma$ was determined for every distinct curve to obtain the best overall agreement. The value for h_{q_m} obtained from our fit was 0.48 which is 20% above the calculated value 0.40.[14]

Figure 2 shows that one can obtain a good matching between experimental and theoretical results. The transient dynamics extends up to about $t=10^{-2}$. The deviations from the master curves for $\phi_q(t)\le 0.2$ mark the onset of that part of the α process which differs from the von Schweidler law. This proves that the experiments follow the predicted master functions. The results also verify the scaling behavior since all curves on the liquid side have the same functional shape, and only the scales differ. The dependence of the scales on φ can then be tested versus the theoretical predictions, and this is done in Figs. 3(a) and 3(b). For the amplitude scale c_σ the theory predicts a square root variation (6b) with respect to the separation parameter σ. This is tested by plotting $(h_q c_\sigma)^2$ (dots) versus the packing fraction φ as is done in Fig. 3(a). The amplitudes used to fit the data closely follow a straight line, and the intersection with the abscissa gives a first determination of the critical value $\varphi_c=0.557$. Similarly, the scale t_σ is predicted to diverge algebraically as in (6a) when approaching the critical point. In Fig. 3(b) we therefore plot ω_σ^{2a} versus φ (solid circles). Again the data points fall close to a straight line, shown by the solid curve, as predicted by the theory. The intersection gives a second value of $\varphi_c=0.559$. In Fig. 3(b) we also show as open circles $\omega_\sigma'^{1/\gamma}$ versus φ. The α-relaxation scale $t_\sigma'=1/\omega_\sigma'$ was taken from the data by that value of time, where the glass structural arrest has decayed to $1/e$, i.e., $\phi_q(t_\sigma')=f_q^c/e=0.30$. Again the experimental data fall on a straight line, given by the dashed curve, and the intersection with the abscissa gives a third value for $\varphi_c=0.560$. Equations (1c) and (6) predict a symmetry for the scales c_σ and t_σ around $\varphi=\varphi_c$ since these only depend on the distance from the critical point. This symmetry is partially verified in Fig. 3 since the points at $\varphi=0.555$ represent the results for $\varphi=0.565$. It is a severe test of the relevance of the analysis, that the three values for the critical point agree so closely. The previous estimate $\varphi_c=0.560\pm0.005$ (Refs 6 and 7) is strongly corroborated by the present analysis.

The appearance of two consecutive relaxation processes with two separate time scales is one of the major predictions of the mode-coupling theory. In order to illustrate this point further we show the time scales t_σ and t_σ' versus φ in Fig. 4. One can clearly see the strong increase of both scales as they approach the critical point. The solid and dashed lines show the theoretical predic-

tions corresponding to the straight lines in Fig. 3(b). At $\varphi=0.48$ the scales differ by one decade while at $\varphi=0.545$ they differ by two decades. So when approaching φ_c the two times separate more and more. Actually it is well known that t_0 also depends appreciably on φ due to hydrodynamic interactions. This dependence can be extracted by fitting the short-time decay to an exponential $\phi_q(t)=\exp(-t/t_0)$. The resulting values for $-t_0\ln(f_q^c)$ are included as a dash-dotted curve in Fig. 4. Figure 5 shows that this fit describes well the first 5–10 % decay

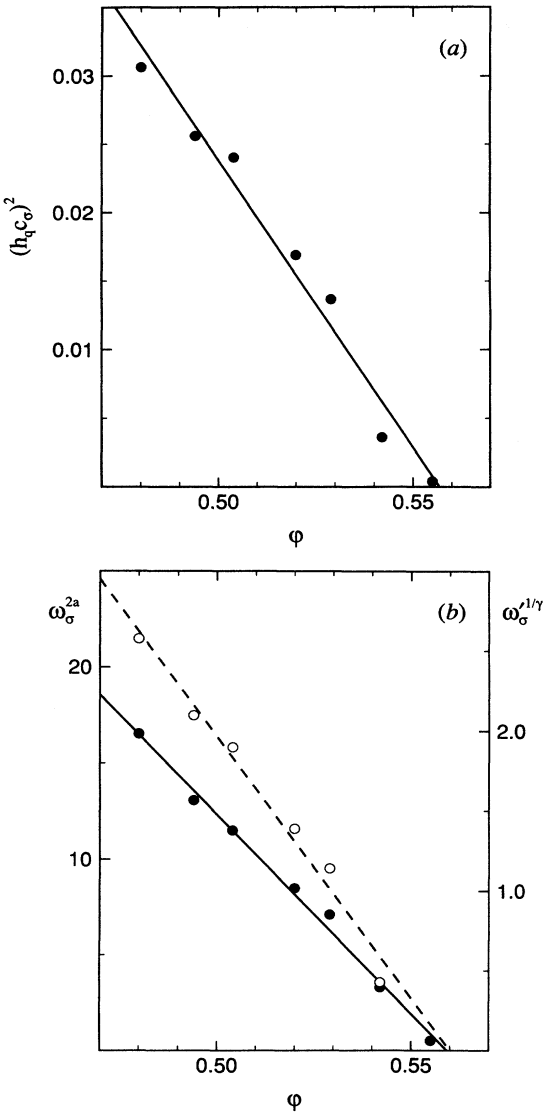

FIG. 3. (a) The dots show the scaling amplitude $(h_q c_\sigma)^2$ vs packing fraction φ obtained from fitting the experimental data. The straight line shows the theoretical prediction in (6b). The intersection with the abscissa gives the glass transition point φ_c. (b) Solid circles show $(1/t_\sigma)^{2a}$ (left scale) and open circles $(1/t'_\sigma)^{1/\gamma}$ (right scale) vs φ as obtained from the experimental data. The theoretical predictions in (6a) and (7b) are indicated by solid and dashed lines, respectively. The intersection with the abscissa gives the critical packing fraction φ_c.

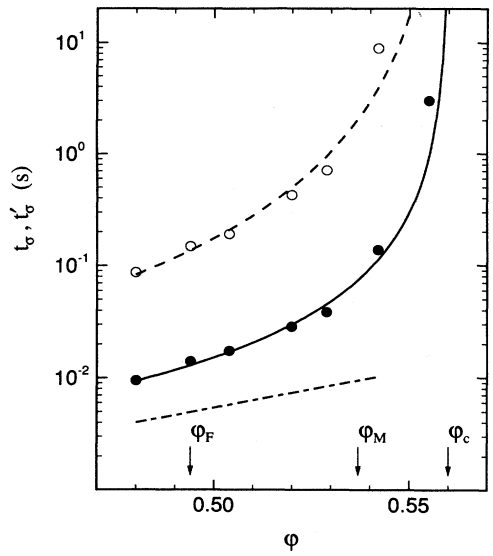

FIG. 4. The two time scales t_σ (solid circles) and t'_σ (open circles) vs φ. The solid and dashed lines show the predicted power laws obtained from the straight lines in Fig. (3b). The dash-dotted curve indicates the density dependence of $-t_0\ln(0.83)$, i.e., where an initial exponential decay crosses f_q^c. φ_c, φ_M, and φ_F denote the glass transition, the melting, and the freezing points, respectively.

of $\phi_q(t)$, but at the level $f_q^c=0.83$ there is already one order of magnitude discrepancy for $\varphi=0.542$. This indicates the importance of the time scale t_σ. For the α-decay process for $\varphi<\varphi_c$ the mode-coupling theory predicts another scaling law: $\phi_q(t)=f_q^c\Phi_q(t/\tau_\alpha)$ with $\Phi_q(t=0)=1$. Here $\Phi_q(\tilde{t})$ is a φ-independent master function and τ_α is the α-relaxation scale. The latter depends sensitively on φ and it is predicted to be propor-

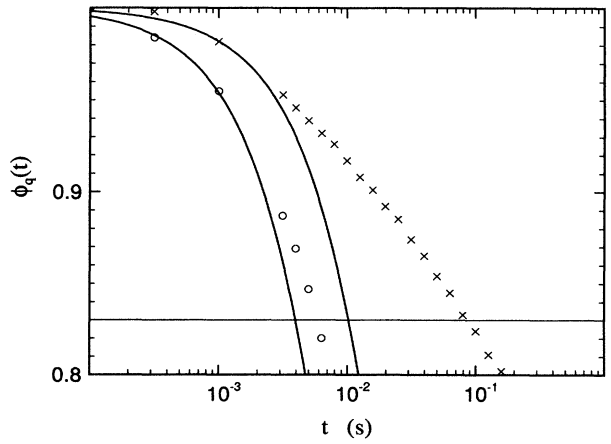

FIG. 5. The solid lines show $\phi_q(t)=\exp(-t/t_0)$ vs t, with t_0 given in Fig. 4, for $\varphi=0.480$ and 0.542, respectively. The symbols refer to the experimental data in Fig. 2. The horizontal thin line indicates the level f_q^c.

tional to t'_σ. The master functions Φ_q are not universal and so far they have not been calculated for the hard-sphere system. But for $t/\tau_\alpha \ll 1$ the scaling result reduces to the von Schweidler behavior (7a), which thus appears also as the short-time part of the α process. A test of the α-relaxation scaling law is shown in Fig. 6. The experimental results are shifted parallel to the abscissa, so that all $\phi_q(t)$ versus t/τ_α agree for $\phi_q(t)=0.3$. If the α-scaling law were valid, all relaxation curves should fall together for $\phi_q(t)<f_q^c$. The data verify the α-relaxation scaling law only for $t \gg t_\sigma$, corresponding to $\phi_q(t)<0.5$. For short times in the β-relaxation region there is a clear deviation from the α-relaxation scaling law. These occur for times much longer than the microscopic transient time t_0. The time t_σ marks the center of these deviations. Also included in Fig. 6, as a solid curve, is a Kohlrausch function $\phi_q(t)=f_q^c \exp[-(t/\tau_\alpha)^\beta]$ with $\beta=0.88$. This value for the Kohlrausch exponent was also found by Bengtzelius for a Lennard-Jones system at $q=q_m$.[10] The value of β is expected to depend strongly on wave vector, and for $q=0.86q_m$ Bengtzelius found $\beta=0.68$. The value of β is, however, sensitive to the time window in which the time decay is analyzed, and the present value is somewhat uncertain. The data for the largest φ value in Fig. 6, for instance, can be fitted for a longer time interval by a Kohlrausch function using a lower value of β.

The predicted asymptotic power-law behavior for the scaling function in (4a) and (4c) is illustrated in Fig. 7, where we show $\log_{10}[|\phi_q(t)-f_q^c|]$ versus $\log_{10}(t)$ for $\varphi=0.542$ and 0.565. The former case gives the function $g_-(\tau)$ while the latter gives $g_+(\tau)$. The power laws which are straight lines with slopes $-a$ and b, respectively, are shown as solid lines in the figure. For the glass side we see that $g_+(\tau)$ after an initial microscopic decay follows the critical decay law (4a) closely, but not perfectly, and then goes over to a constant for long times. An unbiased fit of the data would give a line with some slope $a'<a$. The reason for this is that the true master curve in Fig. 1 differs in the region under discussion, from the short-time asymptotics $1/t^a$. On the liquid side the critical region is not very well separated from the microscopic region. However, there is a clear approach to the von Schweidler law for long times, and this decay can be seen for more than one decade. The exponents a and b can also be obtained by plotting $\log_{10}(h_q c_\sigma)$ versus $\log_{10}(1/t_\sigma)$ and $\log_{10}(1/t'_\sigma)$, which is shown in Fig. 8(a). According to the theory we should find straight lines with slopes a and $ab/(a+b)$, respectively. The theoretical slopes given by the straight lines are reasonably obeyed. There is some discrepancy for the two values of φ closest to φ_c, but these points are sensitive to the precise choice of f_q^c used above. With more data points around $\varphi \approx \varphi_c$ one could find a more optimal value for this parameter. A third cross check is given in Fig. 8(b) where we plot $\log_{10}(1/t'_\sigma)$ versus $\log_{10}(1/t_\sigma)$. The data should fall on a straight line with slope $1+a/b$, which is approximately the case. In this case the dependence on the microscopic time t_0 drops out, and this may explain why the points fall closer to a straight line than in Fig. 8(a). To demonstrate the sensitivity of the preceding tests of the various fits to the correct choice of the exponents, we have added the relaxation curves for $\lambda=0.70$ and 0.82 as dotted lines in Fig. 9. The scales t_σ and $h_q c_\sigma$ are adjusted so as to match the data for $\varphi=0.542$ for the zero, $\phi_q(t^*_\sigma)=f_q^c$, and for $\phi_q(100t^*_\sigma)$. Obviously, the tested 8%

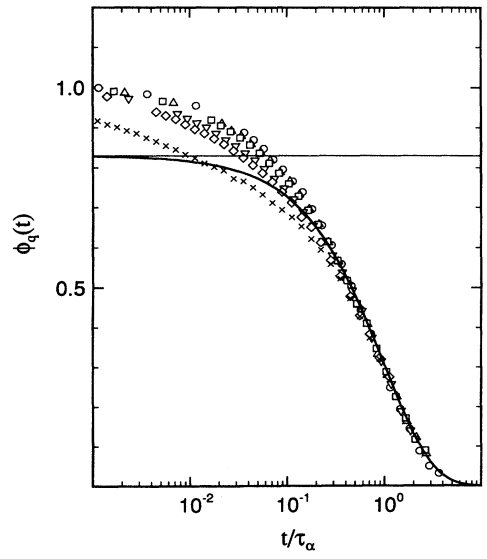

FIG. 6. $\phi_q(t)$ vs t/τ_α for $\sigma<0$. The various symbols refer to those in Fig. 2. The horizontal thin line is drawn at f_q^c. The solid curve represents a Kohlrausch function $\phi_q(t)=f_q^c \exp(-\tilde{t}^\beta)$ with $\beta=0.88$.

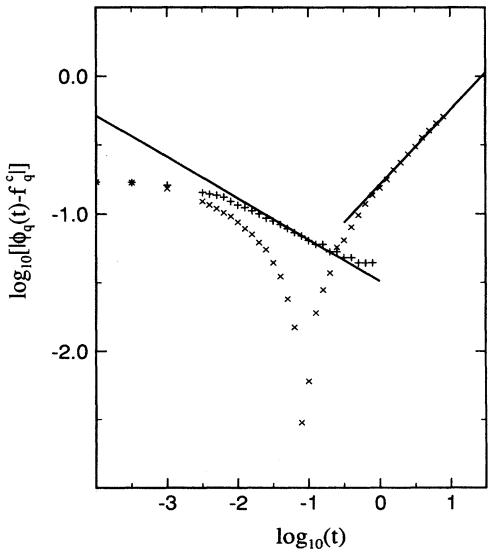

FIG. 7. $\log_{10}[|\phi_q(t)-f_q^c|]$ vs $\log_{10}(t)$ for $\varphi=0.542$ and 0.565 with symbols as in Fig. 2. The straight lines show the predicted slopes $-a=-0.301$ and $b=0.545$, respectively.

change of λ is quite incompatible with the data. We therefore conclude that the analysis confirms the prediction for $\lambda \approx 0.76$ (Ref. 14) with an accuracy of ±4%, which corresponds to an accuracy for the exponents a, b, and γ of about ±10%.

There are also some data for other q values available.[11] According to (1c) they should be related trivially to the ones discussed above. We have checked the behavior for $\varphi = 0.542$ at $q = 0.63 q_m$ and $1.56 q_m$, and find good agreement with the predicted values. However, there is no agreement with the data for $\varphi = 0.494$ for reasons which are presently not clear.

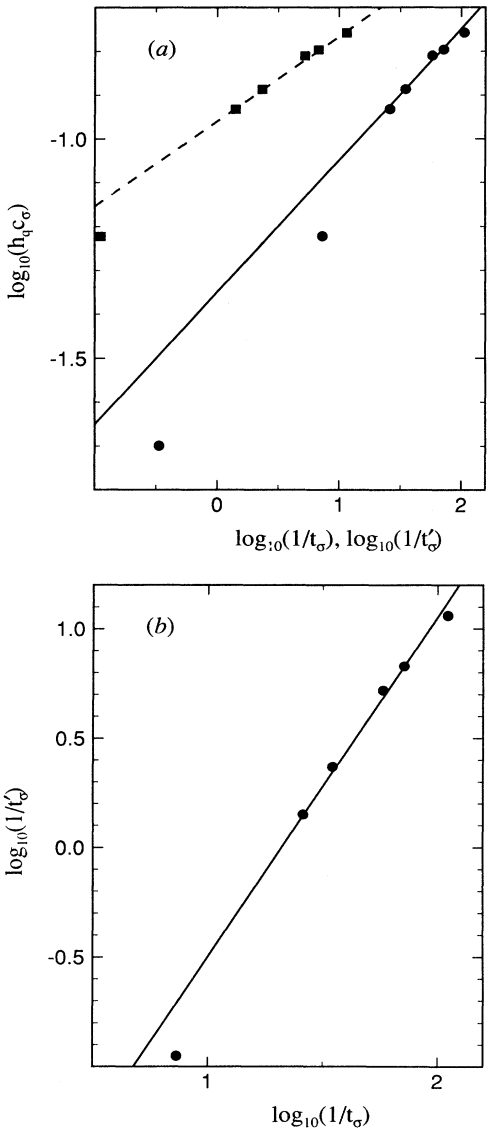

FIG. 8. (a) $\log_{10}(h_q c_\sigma)$ vs $\log_{10}(1/t_\sigma)$ (solid circles) and $\log_{10}(1/t'_\sigma)$ (solid squares). The solid straight line through the former points has slope a, while the dashed line has slope $ab/(a+b)$. (b) $\log_{10}(1/t'_\sigma)$ vs $\log_{10}(1/t_\sigma)$. The solid line has the predicted slope $1 + a/b$.

The analysis above shows that there is a quantitative agreement between the theory and experimental data on an accuracy level of 10% for q at the position of the structure factor peak. This holds for the exponents, the master function and the parameter f_q^c. It should be stressed that to obtain these results only two parameters need to be adjusted, namely, f_q^c and the product $h_q c_\sigma$. Once the former is chosen the time scale t_σ, which includes the unspecified value t_0, can be read off from the intersection of $\phi_q(t)$ with the level f_q^c. The adjusted values f_q^c and $h_q c_\sigma$ can afterwards be compared with actual calculated values. Obviously it would be very worthwhile to extend the experimental work to get data for more q values and also for more values of φ. It is rather surprising to find that the von Schweidler law can account for the data even for very long times where $\phi_q(t)$ have decayed to a rather small value. Conventionally this region of the curves would be fitted with a Kohlrausch decay law $\exp[-(t/\tau_\alpha)^\beta]$, as in Fig. 6. This decay is consistent with (7a) for short times provided one chooses $\beta = b$, but the whole α region cannot in general be fitted by using the exponent b in the Kohlrausch law, as is clear from the data in Fig. 6. The von Schweidler region defines the overlap between the α and the β processes, and it appears as a short-time region of the α process, and as a long-time region of the β process. The length of this common time interval, $t_\sigma \ll t \ll t'_\sigma$, diverges upon approaching the critical point. Within this time interval a useful picture of the relaxation process is provided by the cage effect. In a concentrated system a particle is, at any instant, surrounded by a shell of nearest neighbors which constitutes a cage. These cages represent metastable states with a partially arrested structure, which can have a very long lifetime. For $\sigma > 0$ the β process describes the motion within an arrested structure which is about to break down. In the liquid, $\sigma < 0$, it describes the motion where the cages are almost

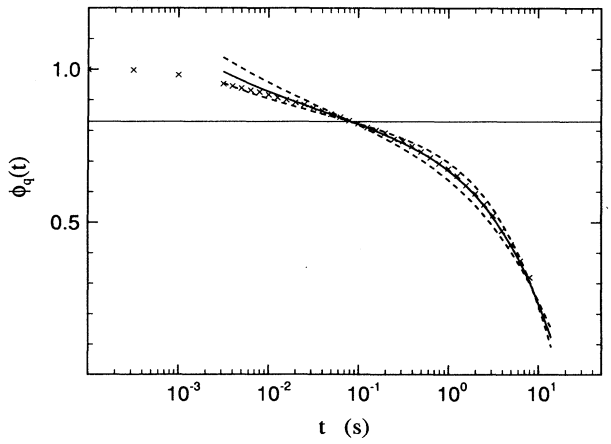

FIG. 9. The symbols show $\phi_q(t)$ vs t for $\varphi = 0.542$, and the solid curve is the theoretical result for $\lambda = 0.758$ as in Fig. 2. The dotted curves correspond to scaling functions for $\lambda = 0.72$ and 0.80.

but not yet completely closed. For $t \ll t_\sigma$, these two types of motion cannot be distinguished as seen in (4a), the liquid appears as frozen. But for $t \gg t_\sigma$ and $\sigma < 0$, the von Schweidler law signals the instability of the apparently arrested structure. The α process describes the complete decay of the structure which appears arrested for $t \ll t_\sigma$. On scale t_σ one cannot decide whether or not the motion is ergodic. This picture of partially trapped particles in metastable states leads directly to the waiting time statistics for the time between events, or lifetimes of the metastable states. The exponents a and b are fractal dimensions of Cantor sets for the event times.[16,17]

The theoretical results used are based on approximations, which treat the glass transition as an ideal one. Necessary extensions of the simple picture alter the transitions to a continuous crossover.[18] For $\varphi \to \varphi_c$ and $\varphi > \varphi_c$ the long-time decay is ruled by hopping processes; they prevent the divergence of the time scales and alter them to finite numbers, essentially to an Arrhenius law.[19] The data discussed for the colloidal system do not show any sign of such effects yet. Since the colloidal particles will continuously exchange momentum and energy with the surrounding solution it is not surprising that barrier hopping processes may be strongly suppressed. In this context it might be interesting to mention that the scaling law analysis of β relaxation in a polymer also was not complicated by the hopping mechanism.[20]

We thank W. van Megen and P. Pusey for several illuminating discussions, and we are grateful that we were allowed to analyze their data prior to publication. This work was supported by the Swedish Natural Science Research Council.

[1]W. Hess and R. Klein, Adv. Phys. **32**, 173 (1983).
[2]W. van Megen and I. Snook, Adv. Colloid Interface Sci. **21**, 119 (1984).
[3]P. N. Pusey and W. van Megen, Nature (London) **320**, 340 (1986).
[4]P. N. Pusey and W. van Megen, in *Physics of Complex and Supermolecular Fluids,* edited by S. A. Safran and N. A. Clark (Wiley, New York, 1987).
[5]I. Livsey and R. H. Ottewill, Colloid Polymer. Sci. **267**, 421 (1989).
[6]P. N. Pusey and W. van Megen, Phys. Rev. Lett. **59**, 2083 (1987).
[7]P. N. Pusey and W. van Megen, Ber. Bunsenges. Phys. Chem. **94**, 225 (1990).
[8]L. V. Woodcock and C. A. Angell, Phys. Rev. Lett. **16**, 1129 (1981).
[9]U. Bengtzelius, W. Götze, and A. Sjölander, J. Phys. C **17**, 5915 (1984).
[10]U. Bengtzelius, Phys. Rev. A **33**, 3433 (1986); **34**, 5059 (1986).
[11]W. van Megen and P. N. Pusey, preceding paper, Phys. Rev. A **43**, 5429 (1991).
[12]W. Götze, Z. Phys. B **60**, 195 (1985); in *Amorphous and Liquid Materials,* edited by E. Lüscher, G. Fritsch, and G. Jacucci (Nijhoff, Dordrecht, 1987), p. 34.
[13]W. Götze, J. Phys. Condens. Matter **2**, 8485 (1990).
[14]J. L. Barrat, W. Götze, and A. Latz, J. Phys. Condens. Matter **1**, 7163 (1989); J. L. Barrat and A. Latz (private communication).
[15]L. Sjögren and W. Götze, in *Dynamics of Disordered Materials,* edited by D. Richter, A. J. Dianoux, W. Petry, and J. Teixeira (Springer, Berlin, 1989), p. 18.
[16]L. Sjögren, Z. Phys. B **74**, 353 (1989).
[17]W. Götze and L. Sjögren, J. Phys. Condens. Matter **1**, 4183 (1989).
[18]S. P. Das and G. F. Mazenko, Phys. Rev. A **34**, 2265 (1986); W. Götze and L. Sjögren, Z. Phys. B **65**, 415 (1987).
[19]L. Sjögren, Z. Phys. B **79**, 5 (1990).
[20]L. Sjögren, in *Basic Features of the Glassy State,* edited by J. Colmenero and A. Alegria (World Scientific, Singapore, 1990), p. 137.